Engineering Solid Mechanics 10 (2022) 341-350

Contents lists available at GrowingScience

Engineering Solid Mechanics

homepage: www.GrowingScience.com/esm

Optimization of wire type and current welding on the strength of welding connection in two types of material testing via response surface methodology

Hery Riyanto[a], Sugito[a*] and Abdul Fikri[a]

[a]*Department of Civil Engineering, Bandar Lampung University, Bandar Lampung, 35142, Indonesia*

A R T I C L E I N F O

Article history:
Received 28 January 2022
Accepted 11 June 2022
Available online
11 June 2022

Keywords:
Hardness
Optimization
RSM
Tensile strength
Welding

A B S T R A C T

The number of types of wire welding that circulate on the market and the development of welding technology, especially related to current welding, create a lack of information related to the quality of welding results for several types of materials. This can cause the strength of the welding connection to not be maximized. Therefore, this study aims to optimize the use of three types of wire welding and three current welding on the strength of the welding connection in two types of material testing using the response surface methodology. Box-Behnken, coupled with the RSM and the desirability function, was used to optimize the strength of the welding connection of the wire types (RD-46, LB-52, and RB-26), and current welding (100, 130, and 160 A) against two types of material testing (IWF-150 and ASTM-A517-G70). The strength of the welding connection observed in response included the tensile strength, Charpy impact-absorbed energy, hardness values in the welding metal and the hardness values in the main metal. Optimization of the strength of the welding connection in this study recommends the application of wire types RB-26, current welding of 100 A, and ASTM-A517-G70 material testing with the highest desirability value of 71.6%. Optimization of tensile strength, Charpy impact-absorbed energy, hardness values in welding metal, and hardness values in main metal by applying this parameter are 575.64 MPa, 110.69 J, 216.75 (HV10) and 126.6 (HV10), respectively. The results proved that an appropriate welding connection strength could be achieved using wire welding types and current welding in material testing.

1. Introduction

We often encounter steel-welding processes in everyday life, ranging from manual and automatic welding techniques. Welding has become a common thing and is often used, for example, in bridge construction, building construction, port construction, pipe manufacturing industry, automotive, transportation, and in children's toys. With the rapid and worldwide development, this welding is slowly being standardized to create good and safe welding results during manufacture and use (Wang et al., 2020; Aris et al., 2019; Chen et al., 2021). Therefore, with various applications and welding methods, proper welding management is needed in planning and calculating so that, at the time of its implementation, it produces a good product and has the expected strength.

To create good and safe welding results, careful and structured preparation is needed for material selection, consumables, welding techniques, and safety procedures. Factors that affect the strength of a welded joint lie in the material to be joined, the filler material for the connection or welding wire, and the connection technique. Weld wire is used as a filler for welded metal to form the strength of the steel joint. The strength of the standard steel area depends heavily on the material to be joined, the welding wire, and the welding process (Kashaev et al., 2018; Zhang et al., 2020; Sathish et al., 2021). Therefore, the proper selection of these parameters must be carefully planned and calculated (Cebro & Sitorus, 2019; Sitrus et al., 2017).

* Corresponding author.
E-mail addresses: sugito@ubl.ac.id (Sugito)

doi: 10.5267/j.esm.2022.6.004

Several research results related to the effect of the welding wire material and the adjustment of the welding machine to the material being welded have been reported. Tušek (2000) reported modeling the melting rate in twin-wire welding. In his paper, he stated that his developed model had already been tested in practice. The results show that they are accurate, simple, and applicable to practice. Furthermore, Sudjadi, et al. (2020) have also reported a study related to the effect of the strength of the electric current in the weld on the tensile strength, where the highest maximum tensile strength is the sample that was achieved with a current of 100 A. The most recent was done by Moi, et al. (2019), which optimizes welding parameters for multiresponse optimization in TIG welding using the response surface methodology (RSM). However, in addition to response surface methodology, optimization can also use artificial neural networks, as done by Familiana et al. (2018). Unfortunately, none of the above studies has studied the strength of welding connections of materials, including IWF-150 and ASTM-A517-G70, which are very common materials, especially in Indonesia.

Unfortunately, until now, no one has reported optimizing the types of wire and current welding on the strength of the welding connection using testing materials, especially IWF-150 and ASTM-A517-G70. Therefore, this study aims to optimize the use of three types of wire and three current welding on the strength of the welding connection in two types of material testing using the response surface methodology. The strength of the welding connection is distinguished by its tensile strength (Ts), Charpy impact absorbed energy (Ecia), hardness values in welding metals (Hwm), and hardness values in main metals (Hmm).

2. Material and methodologies

2.1 Experimental setup

Box-Behnken was used in the design of a series of experiments in this study. In eighteen runs, experimental runs were generated using the Box-Behnken response surface approach, including replication. This number of runs accurately captures the optimal settings and provides significant experimental results (Bakkiyaraj et al., 2022). The design had three independent parameters, including material testing (A), wire welding type (B), and current welding (C). The testing materials used in this study consisted of IWF-150 (1) and ASTM-A517-G70 (2). The type of wire welding used in this study consisted of RD-46 (1), LB-52 (2), and RB-26 (3). The current welding used in this study consisted of 100, 130, and 160 A. Responses correspond to the strength of the welding connection, including tensile strength (MPa), Charpy impact absorbed energy (J), hardness values in the welding metal (HV10), and hardness values in the main metal (HV10).

The IWF-150 testing material used in this study is a wide flange with dimensions of length, width, height, and thickness of 150, 7, 5, and 7 mm, respectively. Furthermore, the ASTM-A517-G70 test material used in this investigation is a steel plate with length, width, and thickness dimensions of 150, 150, and 16 mm, respectively. The voltage used in this study was 28 volts with welding speeds in IWF-150 and ASTM-A517-G70 materials of 125 and 80 mm/minute, respectively. Each test material uses a connection angle of 35°. The process of obtaining samples for testing of the materials tested in this study is presented in Fig. 1.

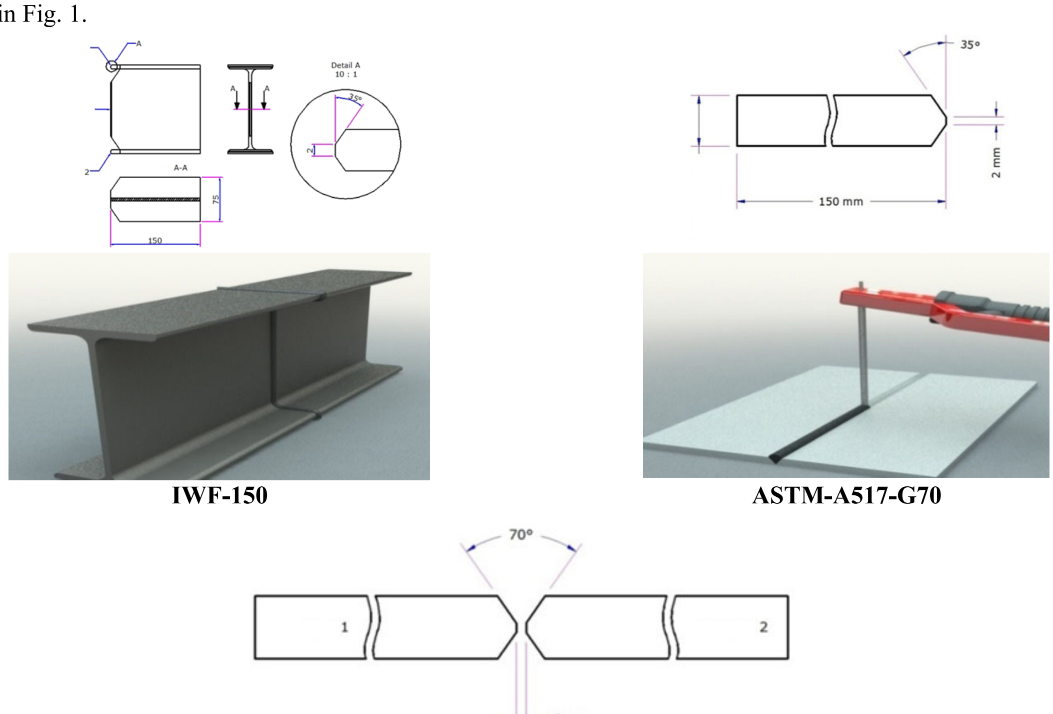

Welding Joining Method

Fig. 1. Material type of sample for testing

The sample is then tested for the strength of the welded joint after welding with three types of wire welding and three types of current welding. Samples were prepared as in Fig. 2 to test the strength of the welded joints. Tensile strength was tested using UTM with a capacity of 200 tons. The impact-absorbed energy of Charpy was measured using the JIS Z 2202 1980 standard (Arifin et al., 2020) with a Charpy impact tester and a hardness value using a Vickers test machine (Nasir et al., 2021) at a predetermined point .

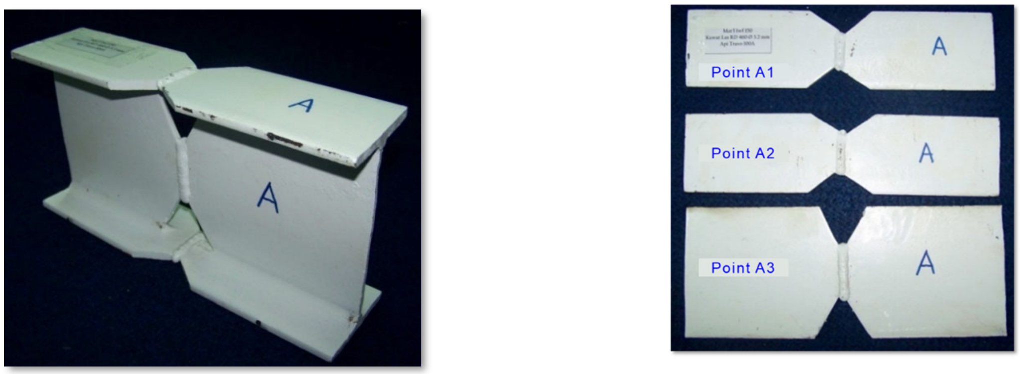

Specimens from IWF-150

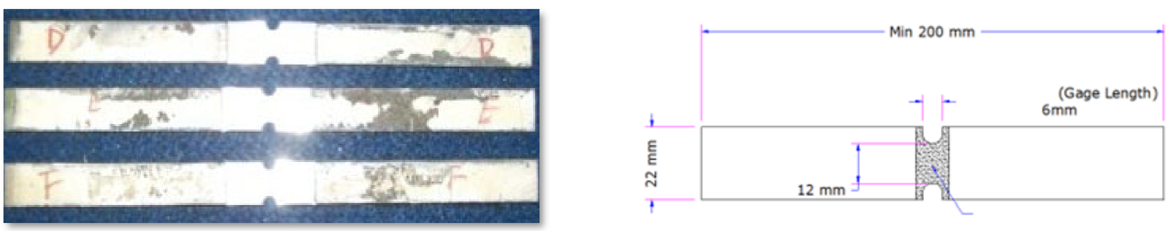

ASTM-A517-G70 specimen from ASTM-A517-G70

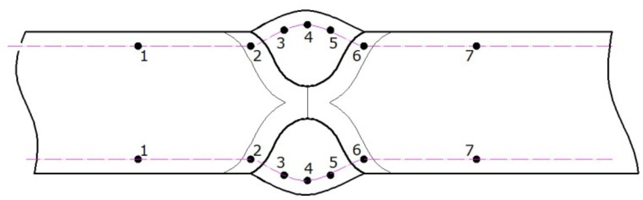

3, 4, 5 = point in welding material

1, 2, 6, 7 = point in main material

Location of hardness measurement point

Fig. 2. Welded joint strength test sample

2.2 Optimization via RSM

The response surface methodology (RSM) predicted the influence of material testing, wire type, and current welding as independent factors on the response strength of welding connections. It addressed the optimization element by determining the optimal welding connection strength. It is possible to apply RSM analysis to estimate the linear interaction and quadratic influence of independent variables on the strength of the welding connection characteristics. The research optimized the combined impact of these factors to minimize or enhance the intended outcomes.

3. Result and discussions

3.1 Regression and establishment

A mathematical function was established to optimize the connection of the welding strength, including tensile strength (MPa), energy absorbed by the charpy impact (Joule at −40 °C), hardness values in the welding metals (HV10) and hardness values in the main metals (HV10). The regression model coefficients were calculated at a confidence level of 95%. The linear statistical model is recommended to predict the response from the evaluation of the type of wire and current welding. Regression models for tensile strength (Ts), charpy impact absorbed energy (Ecia), hardness values in welding metals (Hwm) and hardness values in main metals (Hmm) are given in Equations 1 to 4. Developing the mathematical model for optimization related to this scope is also in line with that generated by Mehdi and Mishra (2020). For the response to tensile strength, the beneficial parameter indicates that the impact of material testing (A) will be a negative effect, the type of wire welding (B), and the applied current welding (C) will be an increased response to it. However, the combined effect of each parameter was not seen for this response. In addition to that, the Charpy impact-absorbed energy response was positively influenced by all parameters (A and B) except the welding current (C), and no combination effect was found between the parameters. On the one hand, the hardness values in the response of the welding metals were positively influenced by all parameters (A, B and C) and a combination effect was found between all parameters (AB, AC, and BC). On the other hand, the hardness values in the response of the main metals were positively influenced by the material testing (A), a combination of the parameter material testing with a type of wire welding (AB) and a combination of the parameter type of wire welding with the welding current (BC). The other parameters have a negative effect on the response to the hardness values in the main metals, including the type of wire welding (B), the welding current (C) and the combination of material testing parameters with the welding current (AC).

$$Ts = 577.72 - 5.83A + 28.58B + 24.83C \tag{1}$$
$$Ecia = 86.61 + 0.1667A + 5.92B - 18C \tag{2}$$
$$Hwm = 194.33 + 12.67A + 12.58B + 9.58C + 8.42AB + 0.9167AC + 0.75BC \tag{3}$$
$$Hmm = 124.83 + 0.3889A - 0.4167B - 0.75C + 0.4167AB - 1.25AC + 0.625BC \tag{4}$$

Eighteen experimental tests were performed to optimize the strength of the welding connection from three parameters, including material testing (A), wire welding type (B) and applied current welding (C). The results show that the maximum tensile strength obtained was 641 MPa on the IWF-150 material test using LB-52 wire welding and 160 A of welding current. The maximum tensile strength obtained in this study was more significant than that obtained by Mehdi and Mishra (2020) in the optimization of process parameters of AA6061 and AA7075 welded joints by TIG+FSP welding using RSM. The maximum energy absorbed by Charpy impact was 127 J in IWF-150 material testing using RB-26 wire welding and 100 A of welding current. Also, the maximum hardness values in the welding metals were 242 (HV10) in ASTM-A517-G70 material tests using RB-26 type of wire welding and 160 A of welding current. The last maximum hardness value in main metals was 128 (HV10) in ASTM-A517-G70 material testing using LB-52 wire welding and 100 A of welding current.

3.2 Effect of current welding and type of welding wire on tensile strength

The effect of current welding on the material's mechanical properties is important to investigate to determine the level of strength, especially for tensile strength (Balasubramanian et al., 2008; Rose et al., 2012). Regression models for the response to tensile strength at low R^2 values (0.3517) indicate a weak fit of the data to the models. The value of R^2 should be close to unity for an ideal model. The results of the statistical analysis for the response to tensile strength are shown in Table 1. Low p-values and high F-values show that the model was not statistically significant. This shows that the combination of parameters does not significantly affect the response to tensile strength of the welding results. However, if we pay close attention to each parameter, we will find that the type of welding wire and the welding current have a significant effect on the tensile strength of the welding results, except for the test material.

Table 1. Statistical data on the tensile strength response

Source	Sum of squares	df	Mean squares	F-value	p-value
Model	17816.92	3	5938.97	2.53	0.0992
A-Material of testing	612.50	1	612.50	0.2611	0.6173
B-Type of welding wire	9804.08	1	9804.08	4.18	0.0602
C- Current welding	7400.33	1	7400.33	3.15	0.0975
Residual	32844.69	14	2346.05		
Total correlation	50661.61	17			

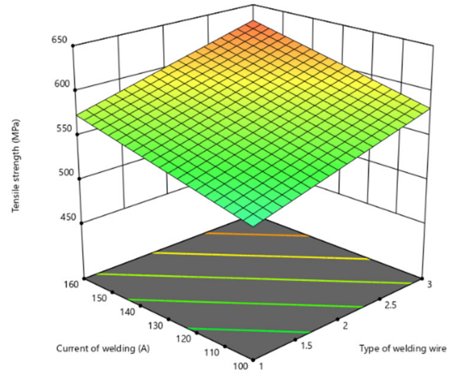

Fig. 3. Response of the surface to tensile strength

The 3D response of surface tensile strength under current welding and the type of welding wire is shown in Fig. 3. It can be seen that increasing the current welding from 100 A to 160 A can significantly increase the tensile strength. Additionally, the use of the welding wire type of RD-46 (1), LB-52 (2), and RB-26 (3) can also significantly increase the tensile strength. It is clear from the graph that the maximum current welding parameters at 160 A and the use of the RB-26 welding wire will produce the maximum tensile strength. Current welding is in line with Razal Rose, et al. (2012) , which state that if the peak current was less than 140 A, there was incomplete penetration and lack of fusion. For peak current greater than 180 A, then weld dropout occurred.

3.3 Effect of current welding and type of welding wire on Charpy impact absorbed energy

The regression models for the response to the energy absorbed by the Charpy impact in the R^2 values (0.6556) indicate a moderate fit of the data to the models. The value of R^2 should be close to unity for an ideal model. The results of the statistical analysis for the response to the energy absorbed by the Charpy impact are shown in Table 2. High p-values and low F-values indicate that the model was statistically significant. This shows that the combination of parameters significantly affects the Charpy impact-absorbed energy response of the welding results. That's because larger Charpy energy is associated with acicular ferrite and ductile failure as a consequence of higher heat (Arista et al., 2021). Furthermore, if we pay attention to each parameter, we will find that the type of welding wire and the welding current significantly affect the Charpy impact absorbed energy of the welding results. However, it is not significant for the testing material used in this study.

Table 2. Statistical data of the Charpy impact-absorbed energy response

Source	Sum of squares	df	Mean squares	F-value	p-value
Model	4308.58	3	1436.19	8.88	0.0015
A-Material of testing	0.5000	1	0.5000	0.0031	0.9564
B-Type of welding wire	420.08	1	420.08	2.60	0.1293
C- Current welding	3888.00	1	3888.00	24.05	0.0002
Residual	2263.69	14	161.69		
Total correlation	6572.28	17			

The 3D response of the surface Charpy impact energy absorbed under current welding and the type of welding wire is presented in Fig. 4. It can be seen that increasing the current welding from 100 A to 160 A can significantly decrease the energy absorbed by Charpy impact. Additionally, using the type of welding wire of RD-46 (1), LB-52 (2) and RB-26 (3) can also significantly increase the energy absorbed by Charpy impact. It is clear from the graph that the minimum current welding parameters at 100 A and the use of RB-26 welding wire will produce the maximum energy absorbed by Charpy impact. This is in line with the research results of K Yasari, et al. (2018), who reported that the electrode RB 26 has the highest tensile strength at 110 A at 184.7 MPa.

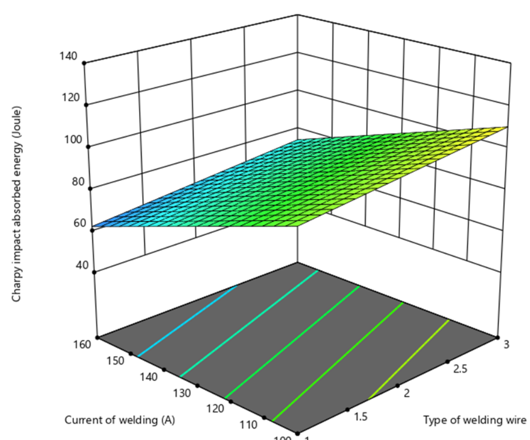

Fig. 4. Response of the surface to Charpy impact-absorbed energy

3.4 Effect of current welding and type of welding wire on hardness values

3.4.1 For welding metal samples

Regression models for the response to the hardness values in welding metal samples in the R^2 values (0.9195) indicate a high fit of the data to the models. The value of R^2 should be close to unity for an ideal model. High p-values and low F-values indicate that the model was statistically significant. The results of the statistical analysis for the response to the hardness values in the welding metal samples are shown in Table 3. This indicates that each parameter (material of testing, type, and welding current) significantly affects the response of the hardness values in the welding metal samples of the welding results.

In addition, the combination of testing material with a type of welding wire has a significant effect on the response of hardness values on welding metals samples. Unfortunately, the combination of testing material with current welding and a type of welding wire with current welding did not significantly affect the response of the hardness values in welding metals samples.

Table 3. Statistical data on the response to hardness values on welding metal samples

Source	Sum of squares	df	Mean squares	F-value	p-value
Model	6754.83	6	1125.81	20.95	0.0001
A-Material of Testing	2888.00	1	2888.00	53.74	0.0001
B-Type of welding wire	1900.08	1	1900.08	35.36	0.0001
C- Current welding	1102.08	1	1102.08	20.51	0.0009
AB	850.08	1	850.08	15.82	0.0022
AC	10.08	1	10.08	0.1876	0.6733
BC	4.50	1	4.50	0.0837	0.7777
Residual	591.17	11	53.74		
Total correlation	7346.00	17			

The 3D response of the surface hardness values in the welding of metal samples under current welding and the type of welding wire is presented in Fig. 5. It can be seen that increasing the current welding from 100 A to 160 A can significantly increase the hardness values on welding metal samples. Additionally, using the welding wire type of RD-46 (1), LB-52 (2), and RB-26 (3) can also significantly increase the hardness values in the welding metal samples. It is clear from the graph that the maximum current welding parameters at 160 A and the use of RB-26 welding wire will produce the maximum hardness values in welding metal samples.

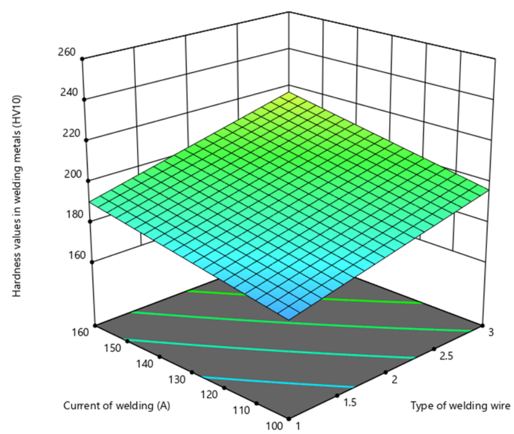

Fig. 5. Response of the surface to hardness values in welding metal samples

3.4.2 For main metal samples

The regression models for the response to the hardness values in the main metal samples in the R^2 values (0. 5037) indicate a moderate fit of the data to the models. The value of R^2 should be close to unity for an ideal model. Low p-values and high F-values indicate that the model was not statistically significant. The results of the statistical analysis for the response to hardness values on the main metal samples are shown in Table 4. This indicates that each parameter (material of testing, type of welding wire, and welding current) and combination of both each parameter (combination material of testing with a type of welding wire, combination material of testing with welding current, combination type of welding wire with welding current) have significantly affected the response to hardness values in the main metal samples of the welding results. Unfortunately, the combination of all parameters did not substantially affect the response of the hardness values in the main metal samples.

Table 4. Statistical data of the hardness value response on main metal samples

Source	Sum of squares	df	Mean squares	F-value	p-value
Model	35.51	6	5.92	1.86	0.1761
A-Material of testing	2.72	1	2.72	0.8559	0.3747
B-Type of welding wire	2.08	1	2.08	0.6550	0.4355
C- Current welding	6.75	1	6.75	2.12	0.1731
AB	2.08	1	2.08	0.6550	0.4355
AC	18.75	1	18.75	5.90	0.0335
BC	3.12	1	3.12	0.9825	0.3429
Residual	34.99	11	3.18		
Total correlation	70.50	17			

The 3D response of surface hardness values in main metal samples under current welding and the type of welding wire is presented in Fig. 6. It can be seen that increasing the current welding from 100 A to 160 A can significantly decrease the hardness values on main metals samples significantly. Additionally, the use of the welding wire type of RD-46 (1), LB-52 (2), and RB-26 (3) can also significantly decrease the hardness values on main metals samples significantly. It is clear from the graph that the minimum current welding parameters at 100 A and the use of the RD-46 welding wire will produce maximum hardness values in the main metal samples.

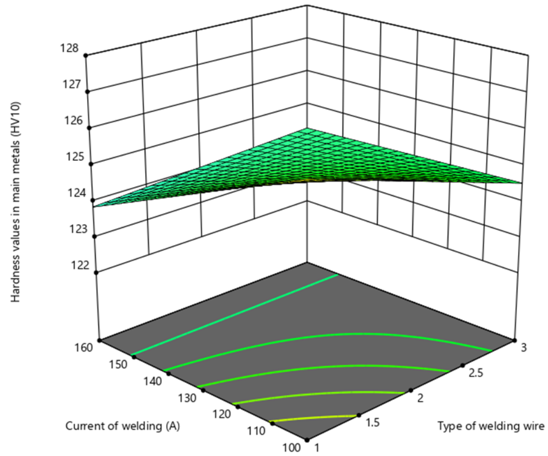

Fig. 6. Response of the surface to hardness values in the main metal samples

3.5 Optimum parameter values

The model's desirability value close to one is the most desirable because it increasingly indicates the importance of optimization accuracy. The desirability value indicates the level of satisfaction of the specified criteria. Based on optimization through RSM, this method shows that the prediction of the most optimal conditions is in a RB-26 wire type, current weldings of 100 A, and ASTM-A517-G70 material testing is recommended as the most optimal formula solution because under this process condition it has the highest desirability value (71.6%). Therefore, it can be concluded that the process conditions with these parameters will produce tensile strength, Charpy impact energy, hardness values in welding metal and hardness values in main metal are 575.64 MPa, 110.69 J, 216.75 (HV10) and 126.6 (HV10), respectively. The results of this study indicate that optimization using RSM can lead to more optimum weld joint strength optimization (Kavitha et al., 2021; Sugito et al., 2022).

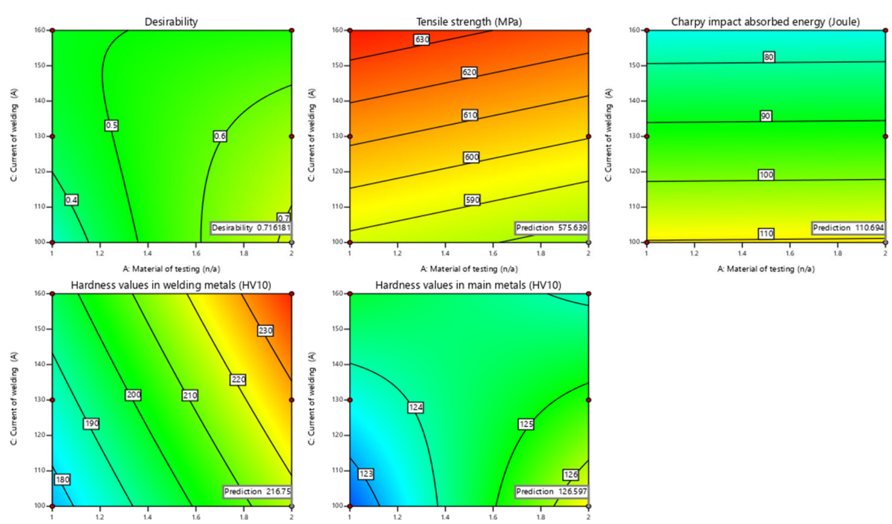

Fig. 7. Optimization of the strength of weld connectivity by desirability function

4. Conclusions

Optimization through response surface methodology using three types of wire (RD-46, LB-52 and RB-26) and three current weldings (100, 130, and 160 A) on the strength of welding connection in two types of material testing (IWF-150 and ASTM-A517-G70) has been extensively investigated. The combination of parameters does not significantly affect the tensile strength response of the welding results. However, each parameter significantly affects the tensile strength of the welding results, except for the test material. The combination of parameters significantly affects the Charpy impact absorbed energy response of the welding results. Furthermore, each parameter has considerably affected the tensile strength of the welding results, excluding the testing material. The test material, type, and welding current significantly affect the response of the hardness values in the welding metal samples to the welding results. Additionally, a combination of testing material with a welding wire has a significant effect on the response of hardness values in welding metal samples except for the combination of testing material with current welding and a type of welding wire with current welding. The test material, the type of welding wire, the welding current, and the combination of both parameters have significantly affected the response of the hardness values in the main metal samples of the welding results except for the combination of all parameters. The response surface methodology combined with the desirability function in this research recommends a formula for wire types RB-26, current weldings of 100 A and ASTM-A517-G70 material testing with the highest desirability value of 71.6%. By applying this formula, the optimization of tensile strength, Charpy impact-absorbed energy, hardness values in welding metal and hardness values in main metal are 575.64 MPa, 110.69 J, 216.75 (HV10) and 126.6 (HV10), respectively. RSM has accumulated a substantial amount of knowledge in a short period of time and with the fewest feasible experiments.

References

Arifin, A., Reza, M., & Wijaya, A. N. P. (2020, May). Development of aluminum matrix composite with hybrid reinforcement using stir casting route. In *IOP Conference Series: Materials Science and Engineering* (Vol. 857, No. 1, p. 012007). IOP Publishing.

Aris, A. A., Maupa, H., Muis, M., & Tabba, M. I. (2019). Effects of government policy, quality of human resources and professional institutions on workforce competitiveness using welding technology as mediating variable. *Journal of Science and Technology Policy Management*, *10*(5), 1121-1151.

Arista, B. V., Flores, I. G., González, C. E. C., Vargas, L. R., & Villasana, J. D. P. (2021). On the effect of Qnet on compressive residual stresses and ductile toughness of dissimilar HAZ in robotic GMAW joints between A572-50 and A36 steels. *The International Journal of Advanced Manufacturing Technology*, *113*(5), 1535-1546.

Bakkiyaraj, M., Gnanasekaran, S., Samuel, S. J. C., Murugan, K., Selvamani, S. T., & Waji, Y. A. (2022). Influence of Process Parameters on Tensile Strength of the Friction Welded AA6063-T6 Joints by Box–Behnken Design Approach. *Advances in Materials Science and Engineering*, *2022*.

Balasubramanian, V., Ravisankar, V., & Madhusudhan Reddy, G. (2008). Effect of pulsed current welding on mechanical properties of high strength aluminum alloy. *The International Journal of Advanced Manufacturing Technology*, *36*(3), 254-262.

Cebro, I. S., & Sitorus, A. (2019). Performance evaluation of a hand tractor to climbing sloping land. *Int. J. Sci. Technol. Res*, *8*(7), 781-785.

Chen, L. K., Yuan, R. P., Ji, X. J., Lu, X. Y., Xiao, J., Tao, J. B., ... & Jiang, L. Z. (2021). Modular composite building in urgent emergency engineering projects: A case study of accelerated design and construction of Wuhan Thunder God Mountain/Leishenshan hospital to COVID-19 pandemic. *Automation in Construction*, *124*, 103555.

Familiana, H., Maulana, I., Karyadi, A., Cebro, I. S., & Sitorus, A. (2018). Characterization of aluminum surface using image processing methods and artificial neural network methods. in *3rd International Conference on Computing, Engineering, and Design, ICCED 2017*, 2018, pp. 1-6.

Kashaev, N., Ventzke, V., & Çam, G. (2018). Prospects of laser beam welding and friction stir welding processes for aluminum airframe structural applications. *Journal of Manufacturing Processes*, *36*, 571-600.

Kavitha, M., Manickavasagam, V. M., Sathish, T., Gugulothu, B., Sathish Kumar, A., Karthikeyan, S., & Subbiah, R. (2021). Parameters optimization of dissimilar friction stir welding for AA7079 and AA8050 through RSM. *Advances in Materials Science and Engineering*, *2021*.

K Yasari, N. M. L. P., Muhayat, N., Triyono, T., & Saputro, Y. C. N. (2018). Microstructural and Mechanical Properties of Underwater Wet Welded SS400 Steel. *Journal of Mechanical Engineering (JMechE)*, (3), 168-179.

Mehdi, H., & Mishra, R. S. (2020). An experimental analysis and optimization of process parameters of AA6061 and AA7075 welded joint by TIG+ FSP welding using RSM. *Advances in Materials and Processing Technologies*, 1-23.

Moi, S. C., Rudrapati, R., Bandyopadhyay, A., & Pal, P. K. (2019). Design Optimization of Welding Parameters for Multi-response Optimization in TIG Welding Using RSM-Based Grey Relational Analysis. In *Advances in Computational Methods in Manufacturing* (pp. 193-203). Springer, Singapore.

Nasir, T., Kalaf, O., Asmael, M., Zeeshan, Q., Safaei, B., Hussain, G., & Motallebzadeh, A. (2021). The experimental study of CFRP interlayer of dissimilar joint AA7075-T651/Ti-6Al-4V alloys by friction stir spot welding on mechanical and microstructural properties. *Nanotechnology Reviews*, *10*(1), 401-413.

Rose, A. R., Manisekar, K., Balasubramanian, V., & Rajakumar, S. (2012). Prediction and optimization of pulsed current tungsten inert gas welding parameters to attain maximum tensile strength in AZ61A magnesium alloy. *Materials & Design*, *37*, 334-348.

Sathish, T., Sevvel, P., Sudharsan, P., & Vijayan, V. (2021). Investigation and optimization of laser welding process parameters for AA7068 aluminium alloy butt joint. *Materials Today: Proceedings*, *37*, 1672-1677.

Sitorus, A., Hermawan, W., & Setiawan, R. P. A. (2017, November). Design and performance of combine corn transplanter powered by hand tractor. In *2017 International Conference on Computing, Engineering, and Design (ICCED)* (pp. 1-5). IEEE.

Sudjadi, U., Wibowo, B., & Hermawan, E. (2020, April). Study of The Effect of The Electric Current Strength of The Weld on The Tensile Strength of The Welded Gas Cylinder Material Joint Capacity of 3 Kg. In *IOP Conference Series: Materials Science and Engineering* (Vol. 839, No. 1, p. 012013). IOP Publishing.

Sugito, S., Alisjahbana, S., & Riyanto, H. (2022). Concrete compressive strength of mix proportioning cockle shell, glass powder and epoxy resin under hot water curing condition through response surface methodology. *Engineering Solid Mechanics*, *10*(3), 263-268.

Tušek, J. (2000). Mathematical modeling of melting rate in twin-wire welding. *Journal of materials processing technology*, *100*(1-3), 250-256.

Wang, B., Hu, S. J., Sun, L., & Freiheit, T. (2020). Intelligent welding system technologies: State-of-the-art review and perspectives. *Journal of Manufacturing Systems, 56*, 373-391.

Zhang, J., Huang, Y., Fan, D., Zhao, J., Huang, J., Yu, X., & Liu, S. (2020). Microstructure and performances of dissimilar joints between 12Cr2Mo1R steel and 06Cr18Ni11Ti austenitic stainless steel joined by AA-TIG welding. *Journal of Manufacturing Processes*, *60*, 96-106.